# Water-soluble silica-overcoated CdS:Mn/ZnS semiconductor quantum dots

Heesun Yang and Paul H. Holloway
*Department of Materials Science and Engineering, University of Florida, Gainesville, Florida 32611*

Swadeshmukul Santra
*Department of Neurological Surgery, University of Florida, Gainesville, Florida 32611*

(Received 17 May 2004; accepted 2 August 2004)

Highly luminescent and photostable CdS:Mn/ZnS core/shell quantum dots are not water soluble because of their hydrophobicity. To create water-soluble quantum dots by an appropriate surface functionalization, CdS:Mn/ZnS quantum dots synthesized in a water-in-oil (W/O) microemulsion system (reverse micelles) were consecutively overcoated with a very thin silica layer (~2.5 nm thick) within the same reverse micellar system. The water droplet serves as a nanosized reactor for the controlled hydrolysis and condensation of a silica precursor, tetraethyl orthosilicate (TEOS), using an ammonium hydroxide ($NH_4OH$) catalyst. Structural characterizations with transmission electron microscopy (TEM) and x-ray photoelectron spectroscopy (XPS) indicate that the silica-quantum dot nanocomposites consist of a layered structure. Owing to the amorphous, porous nature of a silica layer, the optical and photophysical properties of silica-overcoated CdS:Mn/ZnS quantum dots are found to remain close to those of uncoated counterparts. © *2004 American Institute of Physics.* [DOI: 10.1063/1.1797071]

## I. INTRODUCTION

Semiconductor quantum dots (nanocrystals) have a tremendous potential as biomarkers in the fields of molecular/cell biology, medical diagnostics, and targeted therapeutics.[1–6] The high-temperature organometallic procedure-derived core/shell structured quantum dots, where surface passivating layers such as CdS and ZnS are epitaxially grown on the CdSe core, have been found to dramatically enhance the quantum yields of CdSe quantum dots from <10% up to 40%–50%.[7–9] Advanced properties such as higher quantum efficiency and improved photostability in the luminescent semiconductor quantum dots open a promising possibility for the development of a different class of luminescent biomarkers. In addition, luminescent quantum dots (inorganic fluorophores) have advantages over conventional organic fluorophores, since quantum dots have large absorption bands, narrow spectral emission bands, and are photochemically stable. However, luminescent quantum dots synthesized by high-temperature organometallic route yield their poor solubility in water,[2–6,10] indicative of incompatibility with biological environments or aqueous assay conditions.

Several strategies have been pursued to water-solubilize quantum dots with hydrophobic surface. Chan and Nie[2] used mercaptoacetic acid as a coupling reagent with ZnS capped CdSe (CdSe/ZnS) quantum dots. However, it was shown that this surface modification of quantum dots does not ensure persistent bonding, leading to the occurrence of slow desorption of mercaptoacetic acid molecules from the surface of quantum dots, resulting in poor stability of quantum dots in water. As an alternative method, complete encapsulation of individual quantum dots with silica,[3,10] amphiphilic polymer,[4,5] or micelle-forming hydrophilic polymer-grafted lipids[6] has been approached.

The silica coating of colloidal particles has been studied extensively during the past decade with a significant progress particularly in metal nanocrystals[11–14] such as Au and Ag. A wide variety of the applications of silica coating to metal, semiconductor, and inorganic colloidal particles stems from the fact that a silica layer is chemically inert and optically transparent.[15] Additionally, the silica surface can be easily modified with different functional groups by conventional surface chemistry,[16,17] facilitating the solubility of coated colloids in different solvents[17] and the molecular immobilization.[16] The classical Stöber synthesis (base-catalyzed hydrolysis of organometallic precursors, followed by condensation of these hydrolyzed species)[18] and its derivatives[12,15,17] have been used for the successful silica coating on different kinds of colloidal particles. As an alternative synthetic route the silane coupling method,[19] in which silane coupling agent is used as surface primers to render colloidal surface compatible with silicate moieties, has been widely used. The water-in-oil (W/O) microemulsion system in conjunction with the Stöber synthesis has also been used for the preparation of silica-coated cadmium sulfide,[20] silver,[14] and iron oxide[21] nanocrystals.

To date undoped CdSe- or CdTe-based semiconductor quantum dots have been studied exclusively as potential biological labels, along with intensive efforts to water solubilize them. We have previously developed photostable, yellow-emitting ZnS-passivated, and $Mn^{2+}$-doped CdS (CdS:Mn/ZnS core/shell) quantum dots with high quantum yields of 18%–28% via a reverse micelle method,[22,23] in which water nanodroplets present in the continuous oil phase serve as a nanoreactor for the production of semiconductor quantum dots. In this paper, further synthesis of water-soluble silica-overcoated CdS:Mn/ZnS quantum dots is described. The encapsulation of individual CdS:Mn/ZnS quantum dots by a

 

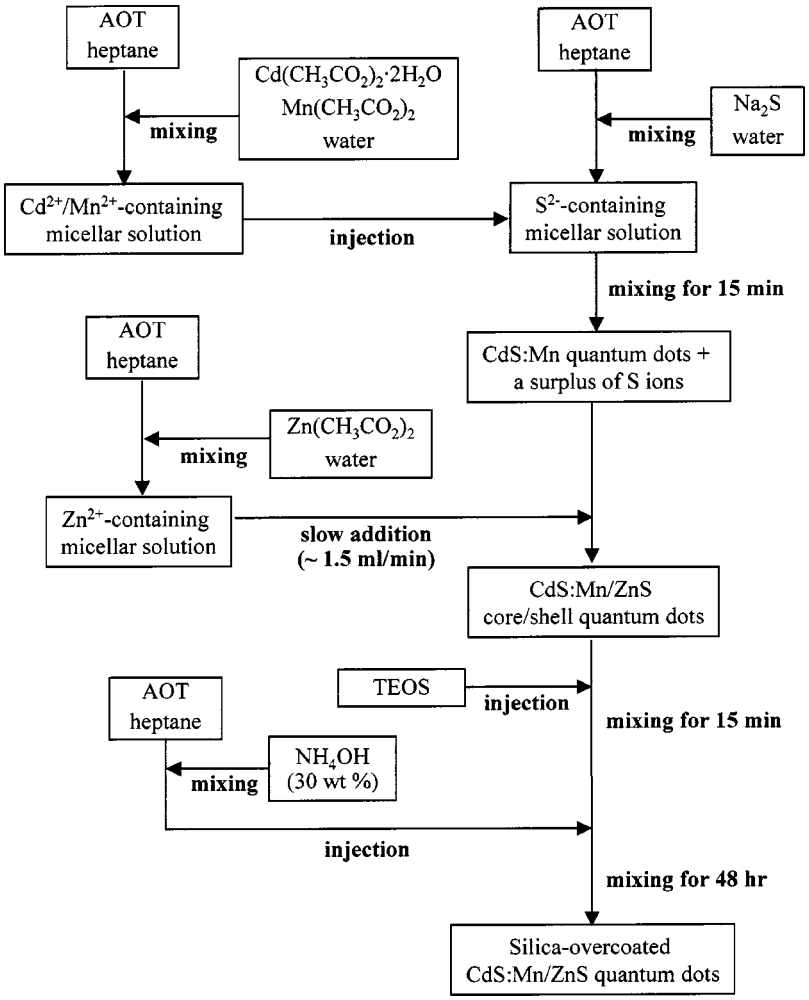


FIG. 1. Schematic flowchart depicting the overall synthesis of silica-overcoated CdS:Mn/ZnS quantum dots.

silica shell was performed by a reverse micellar system, in which the silica shell phase forms by the hydrolysis of tetraethyl orthosilicate (TEOS) in the presence of $NH_4OH$, followed by condensation between hydroxyl groups (—OHs) within water nanodroplets.

## II. EXPERIMENT

$Cd(CH_3COO)_2 \cdot 2H_2O$, $Mn(CH_3COO)_2$, $Na_2S$, $Zn(CH_3COO)_2$, dioctyl sulfosuccinate, sodium salt (AOT), heptane, tetraethyl orthosilicate (TEOS), and $NH_4OH$ (30 wt %) were purchased from Aldrich Chemical Co. Inc. and used as received. Methanol was purchased from Fischer Scientific Co. Distilled deionized water (US Filter) was used for all the preparations.

A typical synthesis of CdS:Mn/ZnS core/shell quantum dots was described in the literature[22,23] and is presented briefly as shown in Fig. 1. After $(Cd^{2+}+Mn^{2+})$-, $S^{2-}$-, and $Zn^{2+}$-containing aqueous solutions are prepared from $Cd(CH_3COO)_2 \cdot 2H_2O$, $Mn(CH_3COO)_2$, $Na_2S$, and $Zn(CH_3COO)_2$, respectively, each solution is stirred with an anionic surfactant AOT/heptane stock solution. CdS:Mn/ZnS quantum dots are formed by mixing $(Cd^{2+}+Mn^{2+})$- and $S^{2-}$-containing micellar solutions for 15 min, followed by the addition of $Zn^{2+}$-containing micellar solution at a very slow rate of ~1.5 ml/min for ZnS shell growth over the CdS:Mn core surface. A surplus of S ions is maintained in the CdS:Mn nanocrystal micellar solution for further ZnS shell growth. The concentrations of $Cd^{2+}$, $S^{2-}$, and $Zn^{2+}$ in water were 0.1*M*, 0.66*M*, and 0.26*M*, respectively [0.048 g of $Cd(CH_3COO)_2 \cdot 2H_2O$, 0.2812 g of $Na_2S$, and 0.264 g of $Zn(CH_3COO)_2$ are used]. The Mn solution concentration in CdS is 2 mol %. The molar ratio of water-to-surfactant (*W*) is 10 for all micellar solutions. The concentration of AOT in heptane is 0.1*M*. After addition of the Zn micellar solution, 3.7 ml of TEOS is injected into CdS:Mn/ZnS micellar solution and mixed for 15 min. The hydrolysis of TEOS and condensation reaction is initiated by adding $NH_4OH$ in the form of micellar solution, which is prepared by mixing 2.2 ml of $NH_4OH$ (30 wt %) with AOT (5.5 g)/heptane (123 ml) stock solution. Since the hydrolysis/condensation reaction is much slower in microemulsion system in comparison to the bulk aqueous solution,[21] quite a long reaction time is required. After polymerization for 48 h at room temperature, transparent micellar solution with silica-overcoated CdS:Mn/ZnS quantum dots is obtained. And silica-overcoated quantum dots are precipitated by addition of a small amount of methanol. After thorough washing with methanol, silica-overcoated quantum dots are solubilized stably in a sodium phosphate buffer solution with *p*H~7. In addition, silica-overcoated CdS:Mn quantum dots without ZnS shell were prepared with the same *W* ratio and Mn concentration.

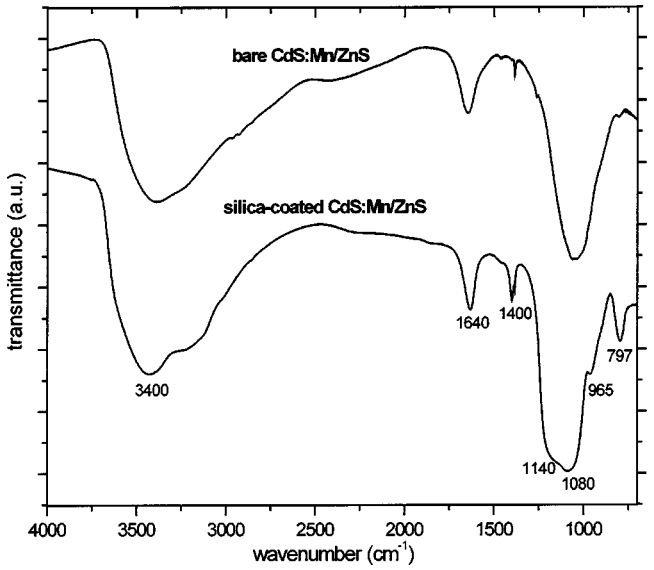


FIG. 2. FT-IR spectra of bare and silica-coated CdS:Mn/ZnS quantum dots.

Infrared (IR) spectra were collected at room temperature on Nicolet MAGNA 760 Fourier transform (FT) IR spectrometer with a nitrogen-purged optical bench. A JEOL 2010F transmission electron microscope operated at 200 kV was used for imaging and direct determination of nanocrystal size. A JEOL JSM 6400 electron microscope operated at 15 kV was used for energy-dispersive spectroscopy (EDS) analysis. A Perkin-Elmer PHI 5100 x-ray photoelectron spectrometer and Mg $K\alpha$ x ray (1253.6 eV) was used for x-ray photoelectron spectroscopy (XPS) analysis. Photoluminescence (PL) emission spectra were collected from 325 nm HeCd laser as excitation sources. And, a monochromatized 300 W Xe light excitation source was used for the monitoring of changes of PL emission intensity as a function of UV irradiation time. Solid-state (dried) nanocrystal films were used for all of these data.

## III. RESULTS AND DISCUSSION

### A. Water-soluble quantum dots and formation of silica shell

The fact that silica-overcoated CdS:Mn/ZnS quantum dots are solubilized and stable in sodium phosphate buffer solution indicates that the quantum dots are surrounded by the silica shell. The presence of hydrophilic hydroxyl groups (Si-OH) (existing in the form of negative charges in aqueous solution) on the silica shell renders the quantum dots water-soluble.[10,12] In contrast, bare (uncoated) CdS:Mn/ZnS quantum dots in the same buffer solution precipitate completely within a short period of time (~2 h).

The FT-IR spectra of bare and silica-overcoated quantum dots are shown in Fig. 2. The signals at 3400 and 1640 $cm^{-1}$ are attributed to adsorbed water molecules, i.e., O-H stretching and H-O-H bending vibrations, respectively. And the peaks at 1400 and 1050 $cm^{-1}$ are presumably attributed to organic groups due to residual AOT or organic solvent. The observation of Si-O-Si and Si-OH bonding by FT-IR spectroscopy is typical of the identification of silica phase. In FT-IR spectrum of silica-overcoated quantum dots, the bands corresponding to Si-O-Si symmetric and asymmetric vibrations are observed at 1140 and 797 $cm^{-1}$, respectively.[24,25] Additionally, the peak at 965 $cm^{-1}$ can be assigned to Si-OH group.[24,26] This FT-IR study indicates that silica phase formed successfully from its precursor (TEOS).

High resolution transmission electron microscopy (HR-TEM) images of silica-overcoated quantum dots are shown in Fig. 3. The silica-coated quantum dots sitting on a normal (carbon-coated) TEM grid are shown in Fig. 3(a). However, the silica shell layer is very difficult to image using a normal TEM grid. This is because the silica layer is amorphous and very thin, making it difficult to distinguish silica from the amorphous carbon film on the TEM grid,[10] even though a relatively thick silica layer with several tens of nanometer scale is easy to observe directly on the normal TEM grid. Instead, a lacey TEM grid, which allows high definition imaging without the effects of underlying support material, was used. For the preparation of TEM samples silica-coated quantum dots in buffer solution were blended with carbon nanotubes dispersed in methanol solution, leading to instantaneous aggregation and subsequent precipitation of the mixture (quantum dots plus nanotubes). And then, a drop of this mixture solution was placed on a lacey TEM grid. By this TEM sample preparation, connected aggregates of silica-coated quantum dots are attached to carbon nanotubes, which are sitting on lacey grid. An aggregated cluster of silica-coated quantum dots attached to a carbon nanotube is shown in Fig. 3(b). The contrast between the light silica shell and the dark CdS:Mn/ZnS quantum dot is apparent. Lattice fringes of ~3.2 nm diameter CdS:Mn/ZnS quantum dots with ~2.5 nm thick silica shell layer can be seen in Fig. 3(c), taken from the dotted area of Fig. 3(b).

The surface sensitivity (few atom layers) of XPS can be used to indicate whether or not the silica covers the outer surface.[7,9,27] XPS spectra from bare and silica-overcoated CdS:Mn/ZnS quantum dots are compared in Fig. 4. It is apparent that the intensities of the photoelectron peaks from Cd, Zn, and S are suppressed on silica-overcoated quantum dots, while the intensity from Si and O is larger, consistent with the presence of a silica surface layer. More quantitative compositional analysis is possible by comparing XPS and EDS data, since XPS is a surface sensitive method and EDS is a bulk method of quantitative compositional analysis.[22] The atomic ratios of Si/Zn from XPS and EDS are determined by integrating the peak areas and dividing by the sensitivity factors. The Si/Zn ratios from EDS and XPS data were obtained to be 8.4 and 16.7, respectively, suggesting that the silica shell has formed on the CdS:Mn/ZnS quantum dot. Besides comparing the ratio of EDS/XPS data, the ratios of Cd photoelectron and Auger electron peak intensities have been compared and further demonstrate that the core/shell structure was achieved in the CdSe/ZnSe (Ref. 27) and CdSe/ZnS nanocrystal systems. The observed intensities for photoelectron and Auger electrons are expressed as follows:

$$I = J_0 N(z)_i \sigma_i Y_{i,n} F(\mathrm{KE}) e^{-z/\lambda(\mathrm{KE})},$$

where $J_0$ is x-ray flux, $N(z)_i$ is the number of $i$ atoms, $\sigma_i$ is absorption cross section for atoms $i$, $Y_{i,n}$ is emission quan-

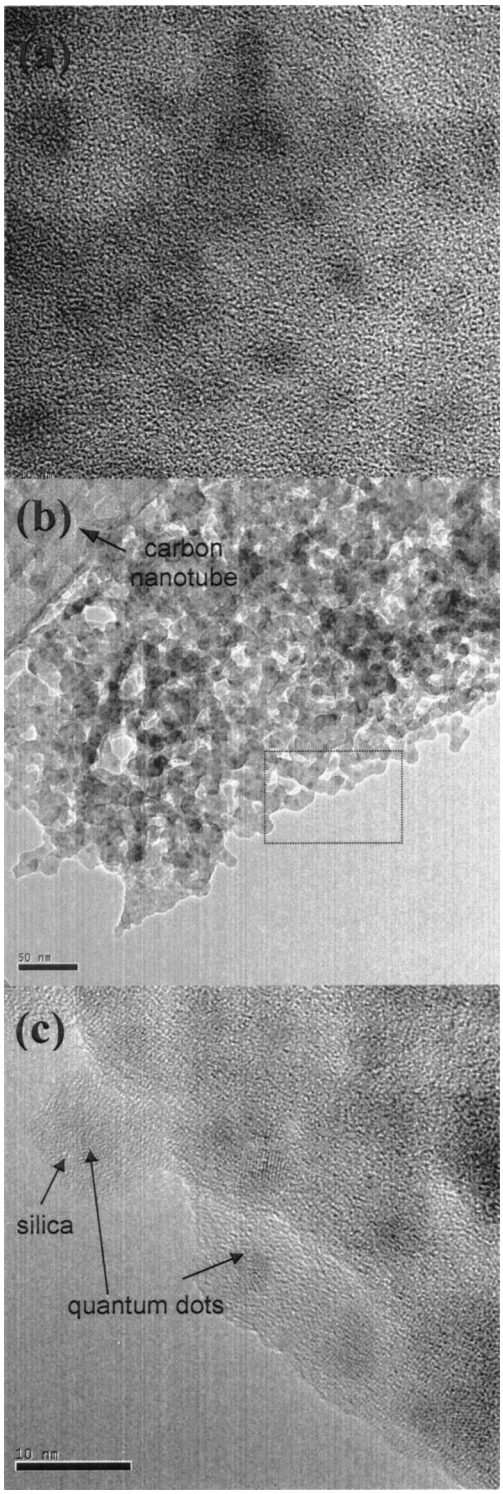


FIG. 3. Transmission electron microscope images of silica-overcoated CdS:Mn/ZnS quantum dots (a) on the normal TEM grid, and (b) and (c) on the lacey TEM grid. Figure 3(c) corresponds to a part of the dotted area in (b). The length bars at lower left corner in (a), (b), and (c) indicate 10, 50 and 10 nm, respectively.

tum yield for process $n$ (photo or Auger electrons) for atoms $i$, $F(\mathrm{KE})$ is an energy-dependent instrument response function, and $\lambda(\mathrm{KE})$ is the energy-dependent escape depth (or attenuation length) for electrons traveling through a core or shell materials. Direct comparison of photoelectron and Auger electron signal intensities from the same atom (e.g., Zn)

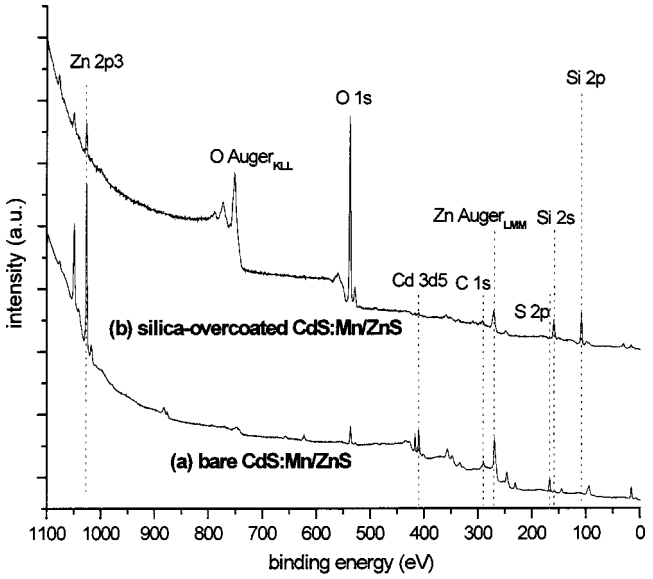


FIG. 4. XPS survey spectra of (a) bare and (b) silica-overcoated CdS:Mn/ZnS quantum dots.

simplifies the above equation, eliminating the $J_0$, $N(z)_i$, and $\sigma_i$ terms. The intensity ratio $I_{\mathrm{silica}}/I_{\mathrm{bare}}$ can be defined, where $I_{\mathrm{silica}}$ and $I_{\mathrm{bare}}$ are the intensity ratios of the Zn photoelectron to Auger electron signals, i.e., $I_{\mathrm{Zn(PE)}}/I_{\mathrm{Zn(Auger)}}$, from silica-coated and bare CdS:Mn/ZnS quantum dots, respectively. The value of $I_{\mathrm{silica}}/I_{\mathrm{bare}}$ is a function of only relative escape depths ($\lambda$) of the photoelectron and Auger electron, and this depth is a function of their kinetic energies and the attenuating materials. The kinetic energies of the Zn $2p$ and Auger (LMM) electrons are 232 and 990 eV, respectively. This energy difference leads to significantly different escape lengths in the silica overcoat on the quantum dots. Specifically, the low energy Zn $2p$ electrons will be attenuated more by the silica layer than the higher energy Zn Auger (LMM) electrons. The observed $I_{\mathrm{silica}}/I_{\mathrm{bare}}$ value of 0.38 is consistent with the presence of a silica overcoat on the CdS:Mn/ZnS quantum dots.

### B. Effects of silica overcoating on PL emission

PL emission spectra, collected from 325 nm HeCd laser excitation, of unpassivated, silica-overcoated, and ZnS-passivated CdS:Mn quantum dots are compared in Fig. 5. Negligible PL emission is observed from unpassivated CdS:Mn, due to the predominance of nonradiative relaxation of photoexcited electron-hole pairs at unpassivated surface sites.[22] Silica-overcoated CdS:Mn quantum dots show higher PL emission as compared to unpassivated dots, but the broad emission can be resolved into two peaks, with a peak at ~470 nm resulting from a surface defect, and the peak at ~620 nm resulting from the $Mn^{2+}$ $^4T_1$-$^6A_1$ transition. In contrast to unpassivated or silica-passivated dots, ZnS-passivated CdS:Mn (CdS:Mn/ZnS core/shell) quantum dots exhibit a very intense and sharp $^4T_1$-$^6A_1$ emission peak at ~600 nm with negligible surface state-related emission, i.e., the ZnS shell is effective in suppressing nonradiative recombination at surface states. Better suppression of surface non-

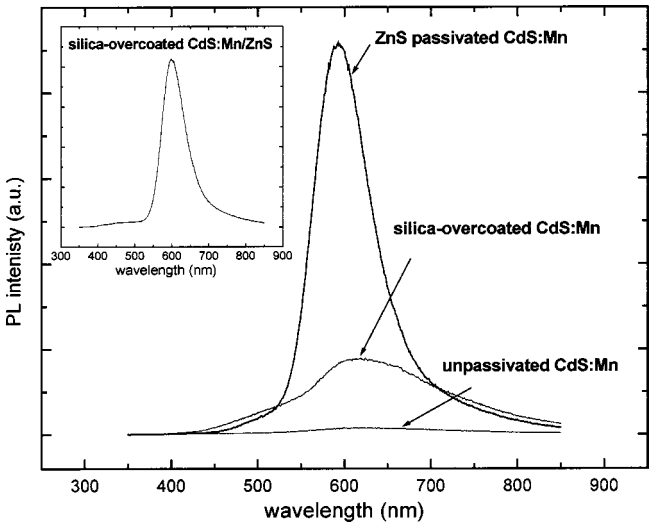


FIG. 5. PL emission spectra of unpassivated, silica-overcoated, and ZnS-passivated CdS:Mn quantum dots using 325 nm HeCd laser excitation. The inset in Fig. 5 is the PL emission spectrum of silica-overcoated CdS:Mn/ZnS quantum dots.

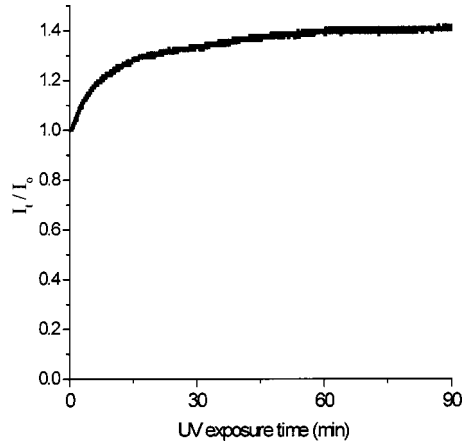


FIG. 6. Variation of 585 nm PL emission intensity of silica-overcoated CdS:Mn/ZnS quantum dots vs time of exposure to 385 nm UV light.

radiative recombination in CdS:Mn/ZnS quantum dots probably results from the fact that the ZnS shell layer is grown epitaxially on the core surface.[22,23] The silica coating of semiconductor nanocrystals can serve to eliminate surface states and consequently enhance PL quantum yield, as reported in silica-coated ZnS:Mn nanocrystals.[28] However, the amorphous silica layer would not form epitaxially and results in a less than complete surface passivation, even though the coverage of silica shell on the CdS:Mn quantum dots appears complete. Besides, significantly broadened $Mn^{2+}$ emission at ~620 nm of silica-coated CdS:Mn quantum dots might be related to the electron-phonon coupling.[22] Since the electron-phonon coupling of quantum dots is determined by the surface characteristics,[29] the coupling strength for silica-coated CdS:Mn quantum dots is larger that than that for ZnS capped cores due to the trapping of electrons and holes at unpassivated surface sites, leading to the broader bandwidth of the emission peak. Finally, the PL emission spectrum from silica-overcoated CdS:Mn/ZnS quantum dots is shown in the inset in Fig. 5, and it is very close to that from bare CdS:Mn/ZnS quantum dots, indicating that silica overcoating does not significantly modify the PL emission properties of CdS:Mn/ZnS quantum dots, which is consistent with the reports on silica-coated CdTe[30] and CdSe/ZnS[10] core/shell quantum dots. Also, intensive studies on silica-coated CdSe/ZnS quantum dots by Alivisatos and co-workers[3,10] showed PL quantum yields of silica-coated quantum dots are about ~5%–18%, which are close to those of uncoated CdSe/ZnS quantum dots. However, Rogach *et al.*[17] demonstrated that their raisin bun-type composites of silica and CdTe or CdSe/CdS nanocrystals exhibited dramatic damping of luminescent intensities as well as significant broadening of emission peaks, as compared to CdTe and CdSe/CdS nanocrystals without silica. These contrast observations of the effects of a silica layer on the PL emission properties are likely to be related to the thickness of silica phase, i.e., ~1–5 nm thick by Aliviastos and co-worker[3,10] versus tens of nanometer thick silica by Rogach *et al.*,[17] suggesting that a thinner silica shell is more desirable to prevent the intensity damping and the peak broadening. Therefore, our silica-overcoated CdS:Mn/ZnS quantum dots with ~2.5 nm thick silica layer are believed to be in a range close to PL quantum yields of uncoated CdS:Mn/ZnS core/shell quantum dots.

The change of 585 nm PL emission intensity of a dried layer of silica-overcoated CdS:Mn/ZnS quantum dots versus time of irradiation by 385 nm UV photons was measured using a Xe light excitation source at room temperature (Fig. 6). Silica-overcoated CdS:Mn/ZnS quantum dots show an increased PL emission intensity of ~40% over the first 60 min, and was stable between 60 and 90 min. We previously reported that the PL emission intensity from bare CdS:Mn/ZnS quantum dots increased as a result of UV irradiation.[23] XPS data revealed that UV irradiation in air atmosphere induces irreversible photochemical reaction (photo-oxidation) of the CdS:Mn/ZnS core/shell quantum dots, producing stable $ZnSO_4$ phase on the ZnS shell surface. This photooxidation product, $ZnSO_4$, serves as an improved passivation layer to further reduce the nonradiative recombination rates. High resolution XPS scans of the S $2p$ peak from bare and silica-overcoated CdS:Mn/ZnS quantum dots are shown in Fig. 7. Both samples were UV exposed in air for 3 h by using a handheld UV lamp providing 366 nm multiband photons with a power density of 1350 $\mu W/cm^2$. On bare CdS:Mn/ZnS quantum dots and two distinct S $2p$ peaks at ~166.5 eV and ~173.8 eV are due to S atoms in the CdS core/ZnS shell and in $ZnSO_4$, respectively.[31] In silica-overcoated CdS:Mn/ZnS quantum dots, however, the S $2p$ peaks are difficult to distinguish due to the attenuation of the S photoelectron signal by the overlying silica shell layer on CdS:Mn/ZnS quantum dot surface. However, even though XPS has the difficulty in detecting S signals in silica-overcoated quantum dots, $ZnSO_4$ is likely to form as a photooxidation product, contributing to enhanced PL emission. The silica phase on CdS:Mn/ZnS quantum dots is amorphous and porous. It is generally believed that the silica layer synthesized from the Stöber chemistry consists of network structures with a relatively large pore size, which are sufficiently large to permit the diffusion of oxygen molecules.[15,16,19] Consequently oxy-

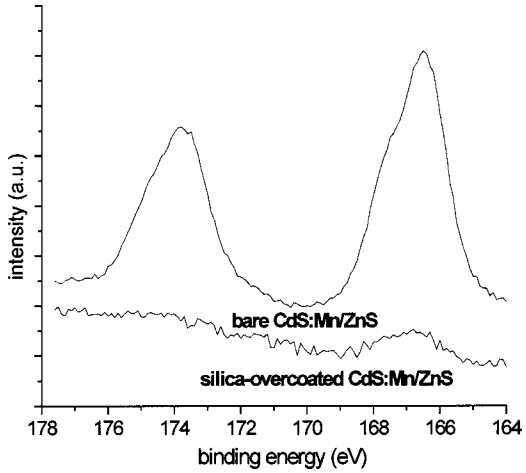


FIG. 7. XPS spectra of bare and silica-overcoated CdS:Mn/ZnS quantum dots after 366 nm UV irradiated for 3 h in air. Both samples were UV-treated by using a handheld UV lamp providing 366 nm multiband photons (see text for discussion).

gen molecules are likely to be accessible to ZnS surface through outmost silica layer, producing photooxidation product, $ZnSO_4$, under UV irradiation.

## IV. CONCLUSIONS

Water-soluble CdS:Mn/ZnS quantum dots were successfully synthesized by silica overcoating. The CdS:Mn/ZnS quantum dot and silica layer were found to be ~3.2 nm in diameter and ~2.5 nm in thickness, respectively. TEM and XPS characterizations confirmed that the CdS:Mn/ZnS quantum dots are overcoated by a silica shell. While the silica surface coating made the quantum dots water-soluble, a silica coating on CdS:Mn/ZnS quantum dots did not significantly modify PL emission properties. Photoluminescence study on silica-coated CdS:Mn quantum dots indicated that nonepitaxially grown amorphous silica layer was not sufficient to passivate the surface of CdS:Mn quantum dots, which is evidenced by weaker/broader emission as compared to ZnS-passivated CdS:Mn quantum dots. Silica-overcoated CdS:Mn/ZnS quantum dots showed enhanced PL emission intensity upon UV (385 nm) irradiation in air atmosphere, followed by excellent photostability during further irradiation (up to 90 min), as a result of diffusion of oxygen molecules through porous silica layer and subsequent photooxidation of ZnS shell surface.

## ACKNOWLEDGMENT

This work was supported by Army Research Office (ARO) and Grant No. DAAD19-01-1-0603.

[1] W. C. W. Chan, D. J. Maxwell, X. H. Gao, R. E. Bailey, M. Y. Han, and S. M. Nie, Curr. Opin. Biotechnol. **13**, 40 (2002).
[2] W. C. W. Chan and S. M. Nie, Science **281**, 2016 (1998).
[3] M. Bruchez, M. Moronne, P. Gin, S. Weiss, and A. P. Alivisatos, Science **281**, 2013 (1998).
[4] X. Y. Wu, H. J. Liu, J. Q. Liu, K. N. Haley, J. A. Treadway, J. P. Larson, N. F. Ge, F. Peale, and M. P. Bruchez, Nat. Biotechnol. **21**, 41 (2003).
[5] D. R. Larson, W. R. Zipfel, R. M. Williams, S. W. Clark, M. P. Bruchez, F. W. Wise, and W. W. Webb, Science **300**, 1434 (2003).
[6] B. Dubertret, P. Skourides, D. J. Norris, V. Noireaux, A. H. Brivanlou, and A. Libchaber, Science **298**, 1759 (2002).
[7] B. O. Dabbousi, J. RodriguezViejo, F. V. Mikulec, J. R. Heine, H. Mattoussi, R. Ober, K. F. Jensen, and M. G. Bawendi, J. Phys. Chem. B **101**, 9463 (1997).
[8] M. A. Hines and P. GnyotSionnest, J. Phys. Chem. **100**, 468 (1996).
[9] X. G. Peng, M. C. Schlamp, A. V. Kadavanich, and A. P. Alivisatos, J. Am. Chem. Soc. **119**, 7019 (1997).
[10] D. Gerion, F. Pinaud, S. C. Williams, W. J. Parak, D. Zanchet, S. Weiss, and A. P. Alivisatos, J. Phys. Chem. B **105**, 8861 (2001).
[11] C. Graf, D. L. J. Vossen, A. Imhof, and A. van Blaaderen, Langmuir **19**, 6693 (2003).
[12] Y. Lu, Y. D. Yin, Z. Y. Li, and Y. A. Xia, Nano Lett. **2**, 785 (2002).
[13] L. M. Liz-Marzan and P. Mulvaney, J. Phys. Chem. B **107**, 7312 (2003).
[14] T. Li, J. Moon, A. A. Morrone, J. J. Mecholsky, D. R. Talham, and J. H. Adair, Langmuir **15**, 4328 (1999).
[15] K. P. Velikov and A. van Blaaderen, Langmuir **17**, 4779 (2001).
[16] S. Santra, P. Zhang, K. M. Wang, R. Tapec, and W. H. Tan, Anal. Chem. **73**, 4988 (2001).
[17] A. L. Rogach, D. Nagesha, J. W. Ostrander, M. Giersig, and N. A. Kotov, Chem. Mater. **12**, 2676 (2000).
[18] W. Stober, A. Fink, and E. Bohn, J. Colloid Interface Sci. **26**, 62 (1968).
[19] M. A. Correa-Duarte, M. Giersig, and L. M. Liz-Marzan, Chem. Phys. Lett. **286**, 497 (1998).
[20] S. Y. Chang, L. Liu, and S. A. Asher, J. Am. Chem. Soc. **116**, 6739 (1994).
[21] S. Santra, R. Tapec, N. Theodoropoulou, J. Dobson, A. Hebard, and W. H. Tan, Langmuir **17**, 2900 (2001).
[22] H. Yang and P. H. Holloway, Appl. Phys. Lett. **82**, 1965 (2003).
[23] H. Yang and P. H. Holloway, Adv. Funct. Mater. **14**, 152 (2004).
[24] G. Hernandez-Padron, F. Rojas, M. Garcia-Garduno, M. A. Canseco, and V. M. Castano, Mater. Sci. Eng., A **355**, 338 (2003).
[25] G. Orcel, J. Phalippou, and L. L. Hench, J. Non-Cryst. Solids **88**, 114 (1986).
[26] J. R. Ferraro and Manghnan Mh, J. Appl. Phys. **43**, 4595 (1972).
[27] C. F. Hoener, K. A. Allan, A. J. Bard, A. Campion, M. A. Fox, T. E. Mallouk, S. E. Webber, and J. M. White, J. Phys. Chem. **96**, 3812 (1992).
[28] A. S. Ethiraj, N. Hebalkar, S. K. Kulkarni *et al.*, J. Chem. Phys. **118**, 8945 (2003).
[29] W. Chen, R. Sammynaiken, R. Wallenberg, and J. Bovin, J. Appl. Phys. **89**, 1120 (2001).
[30] A. Schroedter, H. Weller, R. Eritja, W. E. Ford, and J. M. Wessels, Nano Lett. **2**, 1363 (2002).
[31] National Institute of Standards and Technology (NIST), X-ray Photoelectron Spectroscopy Database 20, Ver. 3.3.